J. Astron. Space Sci. 24(3), 197–202 (2007)

INFRARED COLOR-COLOR DIAGRAMS FOR AGB STARS

Kyung-Won Suh
Dept. of Astronomy and Space Science, Chungbuk National University Cheongju 361-763, Korea
email: kwsuh@chungbuk.ac.kr

(Received July 22, 2007; Accepted July 31, 2007)

ABSTRACT

We present infrared color-color diagrams of AGB stars from the observations at near and mid infrared bands. We compile the observations for hundreds of OH/IR stars and carbon stars using the data from the Midcourse Space Experiment (MSX), the two micron sky survey (2MASS), and the IRAS point source catalog (PSC). We compare the observations with the theoretical evolutionary tracks of AGB stars. From the new observational data base and the theoretical evolution tracks, we discuss the meaning of the infrared color-color diagrams at different wavelengths.

Keywords: stars: AGB and post-AGB, infrared: stars, circumstellar matter, dust: extinction, radiative transfer

1. INTRODUCTION

Asymptotic giant branch (AGB) stars are classified into oxygen-rich stars (M-type Miras and OH/IR stars) and carbon-rich stars (carbon stars) based on photospheric abundance and the chemistry of the outer envelope. Carbon stars are generally believed to be the evolutionary successors of M-type Mira variables that have thin oxygen-rich dust envelopes. When AGB stars of intermediate mass range go through carbon dredge-up processes and thus the abundance of carbon is larger than that of oxygen, oxygen-rich dust grain formation ceases, and the stars become visual carbon stars. After that phase, carbon-rich dust grains start forming and the stars evolve into infrared carbon stars with thick carbon-rich dust envelopes and very high mass loss rates (Iben 1981, Chan & Kwok 1990, Suh 2000).

van der Veen & Habing (1988) used an IRAS color-color diagram as a tool for studying late stages of stellar evolution. They divided the IRAS color-color diagram into eight areas which contain an astrophysically more or less homogeneous group. The infrared color-color diagrams with various infrared wavelength bands provide useful ways to discriminate various types of AGB stars. Suh, Lee, & Kim (2001) presented infrared color-color diagrams of AGB stars using the IRAS and near-infrared data.

In this paper, we make infrared color-color diagrams for AGB stars using the data from the Midcourse Space Experiment (MSX), the two micron sky survey (2MASS), and the IRAS point source catalog (PSC). We compare the theoretical evolution tracks at the new wavelength bands with the observations of AGB stars.

2. NEW INFRARED PHOTOMETRIC OBSERVATIONS

Based on IRAS PSC and Low Resolution Spectrograph (LRS), many investigators have identified different types of the AGB stars using various methods and techniques. Suh, Lee, & Kim (2001)

listed the identified AGB stars in IRAS PSC and presented the infrared color-color diagrams at IRAS bands.

Now, new infrared photometric data are available for the AGB stars. The MSX project (Egan et al. 2003) provides useful photometric data at 8.28, 12.13, 14.65, 21.34 μm wavelength bands. They could be very useful to make new color-color diagrams for AGB stars. Version 2.3 of the MSX Point Source Catalog (PSC) contains 440,483 sources compared to 245,889 sources in IRAS PSC. The 2MASS project (Skrutskie et al. 2006) provides the PSC that contains 500 million sources at J, H, and K bands.

It is difficult to cross-identify the sources because of the different beam size and sensitivity. Lewis, Kopon, & Terzian (2004) found the 2MASS and MSX counterparts for 82 sources from the 134 Arecibo OH/IR stars. Ortiz et al. (2005) found the MSX counterparts for 45 carbon stars.

In this work, we use the MSX and 2MASS PSC data for the AGB stars whose MSX counterparts were found. Using the new colors, we make new infrared color-color diagrams compared with the theoretical evolution tracks.

3. THEORETICAL MODELS

For this paper, we have used the radiative transfer code developed by Ivezić & Elitzur (1997) for a spherically symmetric dust shell. We have performed the model calculations in the wavelength range 0.01 to 36000 μm.

For oxygen-rich stars, we use the optical constants of warm and cool silicate grains derived by Suh (1999). The radii of spherical dust grains have been assumed to be 0.1 μm uniformly. We choose 10 μm as the fiducial wavelength that sets the scale of the optical depth (τ_{10}) and compute models for various optical depths ($\tau_{10} = 0.01, 0.05, 0.1, 0.5, 3, 7, 15, 30$ and 40). For the central star, we assume that the luminosity is $10^4 L_\odot$ and a stellar blackbody temperature is 2500 K for $\tau_{10} \leq 3$ and 2000 K for $\tau_{10} > 3$. We use the warm silicate dust grains for $\tau_{10} \leq 3$ and the cool ones for $\tau_{10} > 3$.

For carbon-rich stars, we use the optical constants of amorphous carbon (AMC) grains derived by Suh (2000) and the optical constants of α SiC grains by Pégourié (1988). The radii of spherical dust grains have been assumed to be 0.1 μm uniformly. We choose 10 μm as the fiducial wavelength that sets the scale of the optical depth(τ_{10}) and perform the model calculations for various optical depths ($\tau_{10} = 0.01, 0.1, 1, 2, 3$ and 5). For the central star, we assume that the luminosity is $10^4 L_\odot$ and a stellar blackbody temperature is 2000 K. For model of carbon-rich stars, we use simple mixture of AMC (90 %) and SiC (10 %) dust grains

For all the models, we assume the dust density distribution is inversely proportional to the square of the distance ($\rho \propto r^{-2}$). The inner shell dust temperature (T_c) is assumed to be 1000 K. The outer radius of the dust shell is always taken to be 10^4 times the dust shell inner radius (R_c). The model SEDs are sensitively dependent on T_c. The temperature is not necessarily the same as the dust formation temperature depending on the physical condition of the pulsating AGB star (Suh 2004).

4. INFRARED COLOR-COLOR DIAGRAMS

We have collected the MSX, 2MASS, and IRAS PSC data of the identified AGB stars as described in section 2. The color index is defined by

$$M_{\lambda 1} - M_{\lambda 2} = 2.5 \log_{10} \frac{F_{\lambda 2}/ZMC_{\lambda 2}}{F_{\lambda 1}/ZMC_{\lambda 1}} \quad (1)$$

where $ZMC_{\lambda i}$ means the zero magnitude calibration at given wavelength (λi). The magnitude

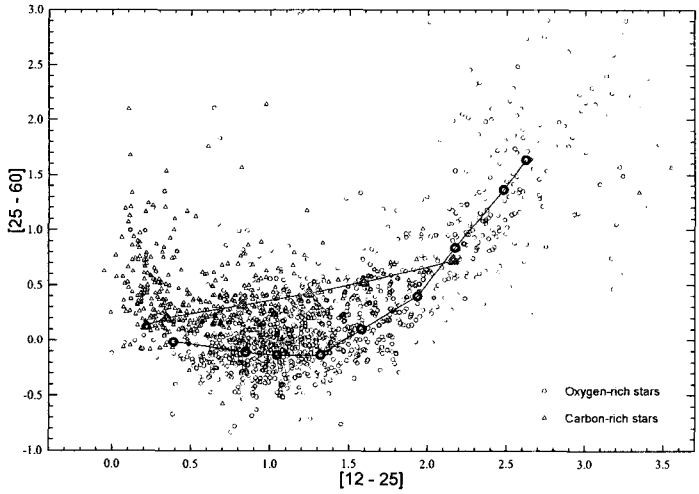

Figure 1. The IRAS color-color diagram for the AGB stars listed in Suh, Lee, & Kim (2001).

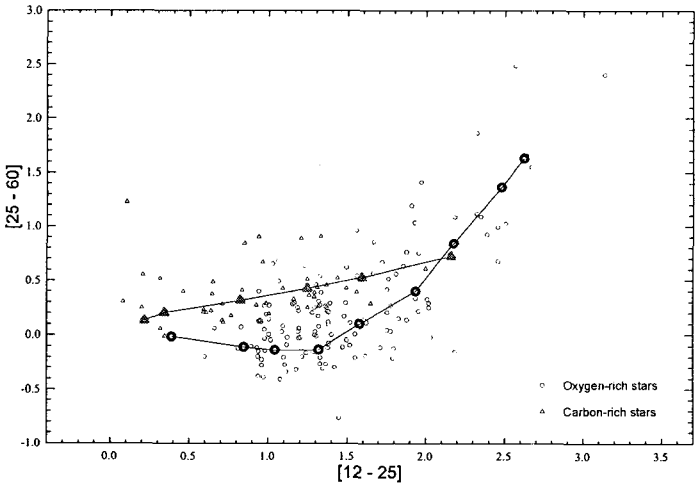

Figure 2. The IRAS color-color diagram for the AGB stars whose MSX counterparts were found.

scale is given in the MSX and IRAS Explanatory Supplement. Sources with good quality at any wavelength were used.

Figure 1 through Figure 6 show the infrared color-color diagrams for AGB stars. The small symbols are the observational data and the large symbols with a line are the models using the opacity functions for a range in dust shell optical depth as we discussed in section 3. The circle symbol represents oxygen-rich stars while the triangle symbols mean carbon-rich stars.

Figure 1 shows the IRAS color-color diagram for the AGB stars using [12–25] versus [25–60],

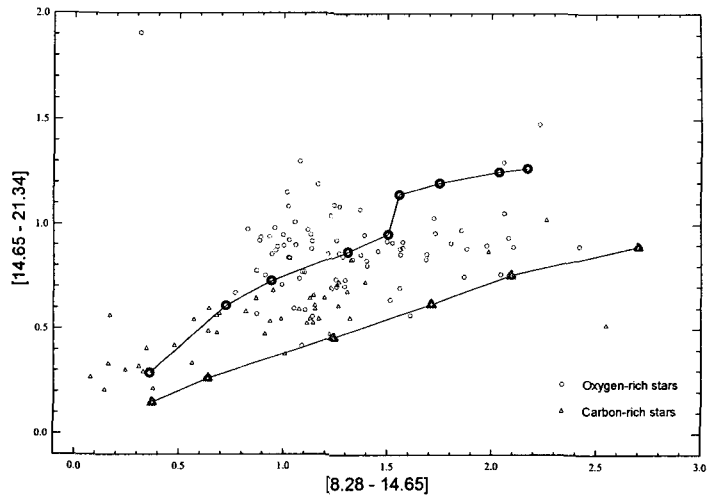

Figure 3. The MSX [8.28–14.65] versus [14.65–21.34] diagram for AGB stars.

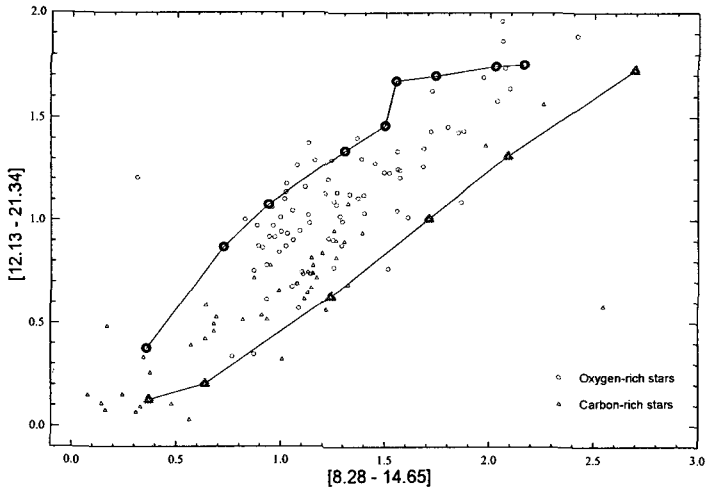

Figure 4. The MSX [8.28–14.65] versus [12.13–21.34] diagram for AGB stars.

as well as the theoretical evolutionary tracks for the thousands of AGB stars listed in Suh, Lee, & Kim (2001). Only a small portion of the stars were found to have MSX counterparts up to now. Figure 2 shows the IRAS color-color diagram only for the stars whose MSX counterparts were found. They are 82 O-rich AGB stars from Lewis et al. (2004) and 45 carbon-rich AGB stars from Ortiz et al. (2005). For those stars, we make new color-color diagrams using the MSX colors.

As the optical depth of the dust shell is increased, the [12–25] color reddens (increases) and [25–60] color reddens very slowly. For carbon-rich stars, both colors show a monotonic increase as the optical depth increases. This is because the opacity for carbon stars is continuous overall in

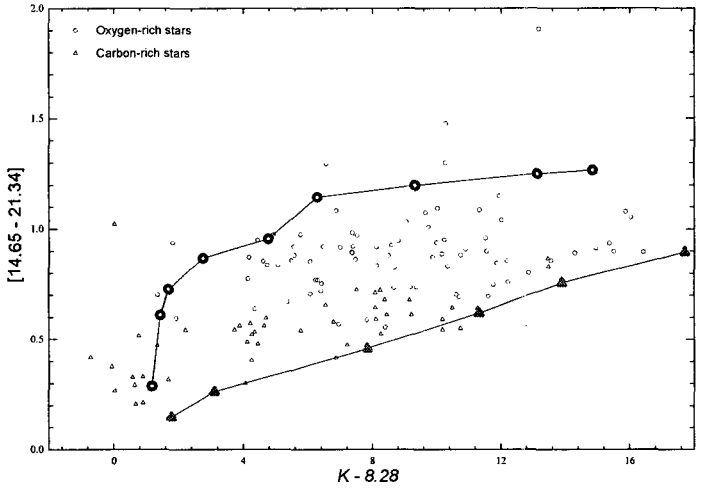

Figure 5. The MSX and 2MASS K – [8.28] versus [14.65–21.34] diagram for AGB stars.

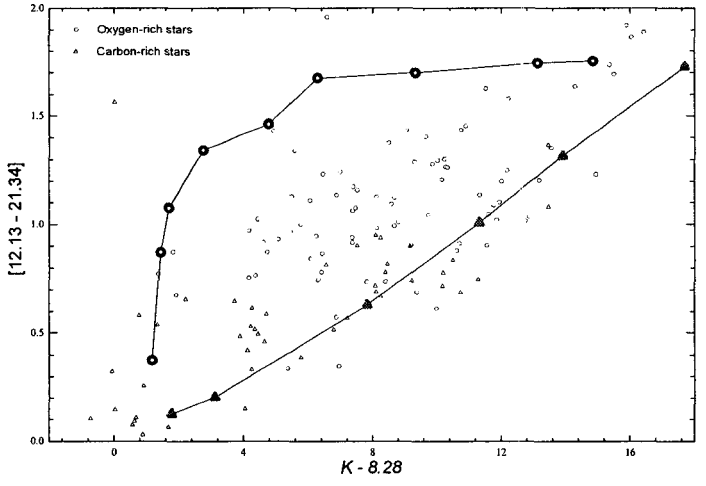

Figure 6. The MSX and 2MASS K – [8.28] versus [12.13–21.34] diagram for AGB stars.

infrared region (Suh 2000). For oxygen-rich stars, the [25–60] color initially decreases because the 20 μm silicate emission feature becomes strong. Then the [25–60] color increases when the 20 μm emission feature becomes weaker when τ_{10} gets from 0.5 to 3 (see Suh 1999).

Figure 3 plots the MSX [8.28–14.65] versus [14.65–21.34] color-color diagram, as well as the theoretical evolutionary tracks for the AGB stars. Figure 4 plots the MSX [8.28–14.65] versus [12.13–21.34] diagram. For carbon-rich stars, both colors show a monotonic increase as the optical depth increases. For oxygen-rich stars, both diagrams show a jump when τ_{10} gets from 3 to 7. When 10 μm silicate emission feature changes to deep absorption, the [14.65–21.34] and [12.13–21.34]

colors increase much faster than the [8.28–14.65] color (see Suh 1999).

Figure 5 plots the MSX K–[8.28] versus [14.65–21.34] diagram, as well as the theoretical evolutionary tracks for the AGB stars. Figure 6 plots the MSX K–[8.28] versus [12.13–21.34] diagram. For oxygen-rich stars, there is a small jump when τ_{10} gets from 3 to 7 with wider range of K–[8.28] color. The reason for the jump is similar to the one described in the last paragraph. In Figures 5 and 6, the observations show higher deviation from the theoretical tracks. Because the K and [8.28] band observations were done at different pulsation phases, the K–[8.28] colors could have some errors.

The position on a color-color diagram of an AGB star changes widely depending on the phase of pulsation (Suh 2004). So the position on the diagram is not fixed. However, for a large sample of AGB stars, the infrared color-color diagram would be a good guide to understand the overall properties.

We have made the four different MSX color-color diagrams for AGB stars. Even if there is no clear separation in the positions of the oxygen-rich and carbon-rich stars, the general distribution of the positions on the diagrams roughly matches the theoretical tracks. When we have a larger sample of the MSX data, we could be able to make more clear conclusion.

5. CONCLUSIONS

In this paper, we have compiled the observations of AGB stars from the MSX, 2MASS, and IRAS PSC data to understand the evolutionary sequence. We have presented infrared color-color diagrams of the stars to compare the observations with the theoretical evolutionary tracks in term of radiative transfer model results. We find that the general distribution of the positions of the oxygen-rich and carbon-rich AGB stars on the diagrams roughly matches the theoretical tracks.

We will be able to identify more AGB stars from the new observations like Akari and Spitzer. When we have the new data with known counterparts of the AGB stars, the color-color diagram could be a more helpful guide to understand the structure and evolution of AGB stars.

ACKNOWLEDGEMENTS: This work was supported by the research grant of the Chungbuk National University in 2006.

REFERENCES

Chan, S. J. & Kwok, S. 1990, A&A, 237, 354
Egan, M. P., Price, S. D., Kraemer, K. E., Mizuno, D. R., Carey, S. J., Wright, C. O., Engelke, C. W., Cohen, M., & Gugliotti, G. M. 2003, Air Force Research Laboratory Technical Report AFRL-VS-TR-2003-1589
Iben, I. 1981, ApJ, 246, 278
Ivezić, A. & Elitzur, M. 1997, MNRAS, 287, 799
Lewis, B. M., Kopon, D. A., & Terzian, Y. 2004, AJ, 27, 501L
Ortiz, R., Lorenz-Martins, S., Maciel, W. J., & Rangel, E. M. 2005, A&A, 431, 565
Pégourié, B. 1988, A&A, 194, 335
Skrutskie, M. F. et al. 2006, AJ, 131, 1163S
Suh, K. -W. 1999, MNRAS, 304, 389
Suh, K. -W. 2000, MNRAS, 315, 740
Suh, K. -W. 2004, ApJ, 615, 485
Suh, K.-W., Lee, J.-W., & Kim, H.-Y. 2001, JA&SS, 18, 15
van der Veen, W. E. C. J. & Habing, H. J. 1988, A&A, 194, 125